Sensors for Smart Grids

Smart Grids Technologies

Francisc Zavoda
Electric Equipment Expertise (EEE)
Research Institute of HQ (IREQ)
Varennes, Canada
e-mail: zavoda.francisc@ireq.ca

Chris Yakymyshyn
FieldMetrics, Inc
Seminole, Florida, USA
e-mail: yakymyshyn@fieldmetricsinc.com

***Abstract*—The Smart Grid will enable the customers to actively decide their energy choices and to accommodate their generation and storage options. The same grid will provide higher reliability and consistent power quality, which are required by our digital economy, by optimizing the use of assets and the grid operation. The future power grids will come into reality by enabling intelligent communication across sensing, measurement, and control layers that are embedded into the existing power systems. This paper discusses the results from tests performed on two sensors, a combined voltage and current sensor and an optical voltage sensor.**

Keywords-Smart Grid; Distribution Automation; Volt & VAR Control; Fault Location; Power Quality; monitoring; sensor; accuracy, magnitude, phase angle.

I. INTRODUCTION

The Smart Grid will enable the customers to actively decide their energy choices and to accommodate their generation and storage options. The same grid will provide higher reliability and consistent power quality, which are required by our digital economy, by optimizing the use of assets and the grid operation. The future power grids will come into reality by enabling intelligent communication across sensing, measurement, and control layers that are embedded into the existing power systems.

Smart distribution systems will increasingly be dependent on monitoring of the system conditions for both real time management and improved maintenance strategies [1]. Integrated distribution monitoring systems will require various types of sensors and transducers to help understand system conditions and respond to disturbances affecting it. Voltage and current monitoring will be critical for a large number of applications [2]. Specific sensor requirements will include support for:

- Advanced voltage control functions for voltage optimization, voltage reduction, Volt/VAR control,
- Load current monitoring for reconfiguration strategies, asset management and fault location applications,
- Protection and reconfiguration applications (fault current monitoring, coordination of protection characteristics, etc.),
- Waveform acquisition for fault location and other diagnostic applications including incipient fault detection and location,
- Harmonic monitoring for power quality assessments and other diagnostic applications.

Nowadays, several manufacturers offer performing sensors to improve network performance.

The paper is divided into several sections. Section II discusses the need for new sensors. Sections III and IV describe optical sensor techniques. Section V describes the details of the sensors that were tested. Section VI describes the test methods used. Section VII presents the test results. Section VIII provides conclusions.

II. SMART GRID AND SMART DISTRIBUTION

Today, advances and falling prices of the communication and control technologies, allow their embedding into distribution grid and use for grid monitoring and remote control of major distribution equipment, (switches, capacitors banks, reclosers and voltage regulators), thus replacing the old Distribution Automation (DA), consisting mainly in automatic operation of medium voltage (MV) equipment.

A better knowledge of what is happening in the power system is crucial for an improved distribution grid management. New technologies such as sensors, IEDs, software and telecommunication can provide data required by smart distribution applications to improve the power system efficiency through utility's business needs. It is a necessary feedback loop to improve the distribution system performance.

The new way of thinking and operating the Smart Grid created the premises for an integrated distribution monitoring system, based on sensors and Intelligent Electronic Devices (IED) capable of providing accurate and reliable data required by new smart distributed applications.

III. SENSORS

For Smart Grid and Smart Distribution (SD) applications, vendors propose new "Smart Sensors", which can work autonomously, when equipped with a communication interface, or in combination with IEDs. Among them,

 ISBN: 978-1-61208-259-2

voltage and current optical sensors offer a number of major advantages, but the speed of their integration into the grid depends on price reduction.

IV. OPTICAL SENSORS

Conventional methods to monitor overhead electrical lines use iron core instrument transformers, which are not easy to mount because of their significant size and weight, and can present safety constraints to personnel as well as to the interconnected equipment. The physical hazards associated with conventional iron-core devices, when coupled with the complexity of installation, have typically precluded their use within medium-voltage distribution systems.

The Optical Sensors [3] represent a significant improvement over conventional iron-core instrument transformers or Rogowski coils. These sensor devices are positioned for use in switchgear, power distribution, electronics and medium voltage applications (< 37 kV) where the conventional current and voltage transformers may be undesirable due to space and weight concerns.

A. Optical Current Sensor (OCS)

The technology used by optical current sensors is based on the Faraday effect. When a linearly polarized light travels through a transparent material that is exposed to a magnetic field, its plane of polarization rotates (see Figure 1). In sensor systems that exploit the Faraday Effect, a sensor assembly is placed into a magnetic field. By monitoring the rotation of the incident polarization state, a direct measurement of the magnetic field intensity, and consequently the associated current, can be inferred.

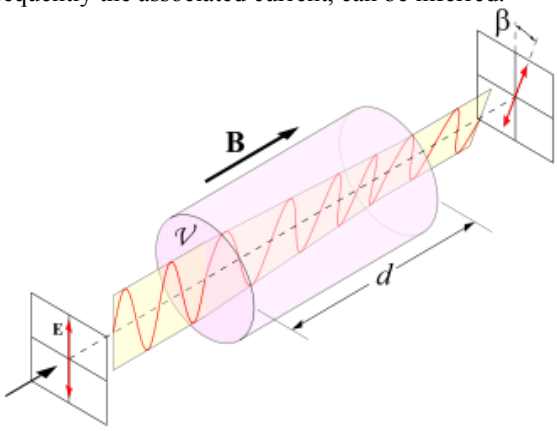

Figure 1. Faraday effect (source Wikipedia)

Currently, there are several types of optical current sensors on the market, which use radically different technologies.

Some of them use either bulk optical crystals or long lengths of optical fiber, coiled around a current-carrying conductor. When an optical path completely encircles a conductor, as is the case of coiled optical fiber sensors, a numerical integration can be performed about the optical path that directly relates the Faraday rotation to the current flowing through that optical path. The measurement sensitivity is dependent on the number of optical fiber turns around the conductor being monitored.

The sensors utilizing bulk glass take advantage of the Faraday Effect exhibited by the bulk glasses [4]. The sensor can be fabricated from materials, which are more sensitive to the influencing magnetic field than those used in coiled optical fiber sensors.

Fiber optic magneto-optic field sensors [5] use ferromagnetic materials more sensitive than materials used in simple fiber optic cable or bulk-optic crystals. The straightforward result is that the sensor requires much smaller Faraday rotator to measure a given magnetic field strength, and offers versatility in physical size and the range of measurement properties.

B. Optical Voltage Sensor (OVS)

The OVS technology [6] is based on the Pockels effect. It is used to make Pockels cells, which are voltage-controlled wave plates (see Figure 2).

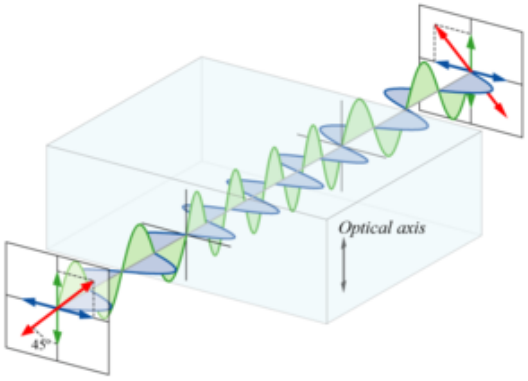

Figure 2. Half wave plate (source Wikipedia)

When a steady electric field is applied to certain electro-optic materials, their refractive indices change, roughly in proportion to the strength of the applied field. The Pockels effect occurs only in noncentrosymmetric optical crystals, such as lithium niobate or gallium arsenide. In combination with a polarizer, Pockels cells can be used as an extremely fast shutter that can respond in nanoseconds. In sensor systems that exploit the Pockels effect, a sensor assembly is placed into an electric field. When polarized light is projected through the Pockels cell that is in this voltage field, the state of polarization of the light traveling in the crystal is rotated. From the measured polarized light rotation the voltage across the crystal can be determined.

V. SENSORS UNDER TEST

Both sensors used in this study, the MetPod [7] and the Optical Voltage Transducer (OVT), were rated for 25kV class operation. Prior to frequency response testing, the prototype devices passed dielectric type testing [8,9]. This included a dry AC withstand test at 50 kV for 1 minute, followed by BIL testing of 15 full wave impulses (1.2 x 50 microseconds) at 150 kV peak, along with two or more chop wave impulses (1.2 x 3 microseconds) at 175 kV peak. Both

 ISBN: 978-1-61208-259-2

polarities were applied in the BIL tests. Thermal cycling was performed in an insulating temperature chamber while the device was energized with high voltage, or simultaneously with high voltage and moderate current. The thermal ramp rate was kept at <30 ºC/hour to allow the unit under test to thermally equilibrate with the ambient temperature in the test chamber.

1) MetPod/Combined Voltage & Current Transducer (CVCT)

The MetPod (see Figure 3) is a self-powered sensor solution that combines a voltage sensor, a current sensor and a power supply to provide output signals suitable for interfacing with IEDs. As shown in Figure 3, the MetPod uses a hollow core composite silicone polymer insulator to support a high voltage conductor. The opposite end is tied to neutral. An optical fiber carries digitized current and voltage data from the MetPod to an interface module, where it is converted back to either low voltage signals or 120V and 1A signals suitable for interfacing with a variety of power quality measurement devices.

Figure 3. MetPod sensor

The current sensor approximates Ampere's law by integrating the spatial magnetic field around a closed path that encircles the high voltage conductor using a plurality of point sensors. This approach generates a sensor output that is independent of: conductor position within the sensor window; conductor size; current density distribution within the conductor; or magnetic field perturbations caused by adjacent phases or nearby ferrous objects. The use of an air core permits an open slot on one side of the current sensor that allows installation without breaking an existing high or medium voltage conductor.

The voltage sensor uses a precision impedance divider collinearly located near a second impedance string that supplies AC current to an integrated power supply. Because of the relatively low impedance of the voltage divider (<10 Megohms at 60 Hz), and the electrostatic shield provided by the second impedance string, the voltage measurement is insensitive to external electric field perturbations caused by adjacent phases, pollution or ice on the insulator surface, etc. The hollow insulator is pressurized to 15 psi with dry nitrogen gas.

At the high voltage end of the MetPod, two 24-bit A/D converters digitize and interleave the sensor signals, while providing a signal bandwidth of 20 kHz. The single digital stream is coupled onto a conventional multimode fiber and transferred out of the neutral end of the MetPod. The analog signals that are reconstructed at the interface module have a fixed group delay of approximately 650 microseconds relative to the high voltage conductor. Due to the interleaved sampling, the relative phase error between the voltage and current signals is <0.2 degrees at 60 Hz.

As declared in the sensor's technical specification, the voltage and current measurements meet 0.3% accuracy or better over a temperature range of -20 ºC to +60 ºC. The current sensor's rated current range extends from 200 A to 10,000 A. In all cases, the current sensor is not damaged by currents with crest values as high as 20,000 A.

2) Optical Voltage Transducer (OVT)

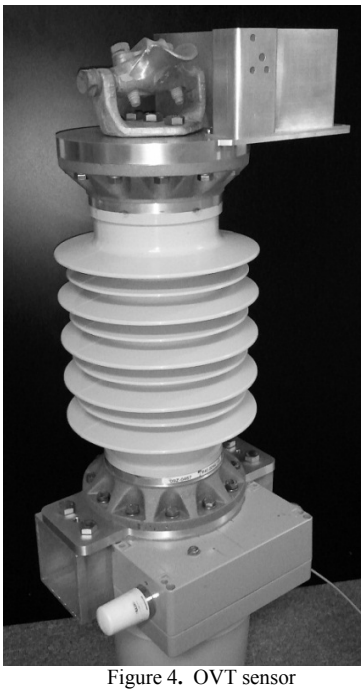

Figure 4. OVT sensor

The OVT (see Figure 4) has the same physical footprint as the MetPod. A collimated light source located at the high voltage end is circularly polarized before passing through an aperture. The optical beam then passes through one or more optical crystals located along the length of the hollow core insulator. Each electro-optic crystal modulates the state of polarization of the light in direct proportion to the voltage drop across that crystal. Provided the modulation depth is kept small, the final state of polarization is a linear sum of

 ISBN: 978-1-61208-259-2

the modulation imparted by each crystal along the vertical optical beam path. This provides an excellent approximation to the line integral of the electric field between high voltage and neutral, which is the definition of potential difference. The polarization-modulated optical beam is sampled by two photodiodes fed by the orthogonal outputs of a polarizing beamsplitter. The two detected signals undergo separate normalization and temperature compensation prior to being differenced to create the final output signal. Differencing removes common-mode noise that may arise from a variety of sources. The analog signal is digitized and transferred onto standard multimode tele-communications optical fiber. The resulting sensor system operates within a factor of 2 of the shot noise limit, with a signal bandwidth of >20 kHz.

A co-located impedance string feeds the integrated power supply to energize the light source at the high voltage end, and a second power supply at the neutral end to power the optical receiver electronics and digitizer.

The OVT provides 0.3% accuracy from 80% - 120% of rated line voltage, over a temperature range of -20 ºC to +60 ºC. The system bandwidth is >20 kHz.

VI. EXPERIMENTAL SETUP

The measurement of the harmonic response of the MetPod and the OVT was performed using two separate setups.

A. Voltage Measurement Setup

As shown in Figure 5, the MetPod voltage response and the OVT response were evaluated by applying a harmonic tone superimposed on a 60 Hz carrier signal. One arbitrary waveform generator (HP 33120A), operating at 60 Hz, was used to phase-lock a second HP 33120A operating at a harmonic of 60 Hz. The amplitude of each generator was independently adjustable. The two sinusoids were combined and amplified by a 2400W power amplifier, which drove the secondary winding of a 300:1 Potential Transformer. The high voltage signal was applied to the device under test (DUT), and monitored using a reference divider having a bandwidth of >100 kHz. The low voltage output of the interface module was amplified by a precision amplifier with a gain of G=20. An identical amplifier was used to amplify the output of the reference divider.

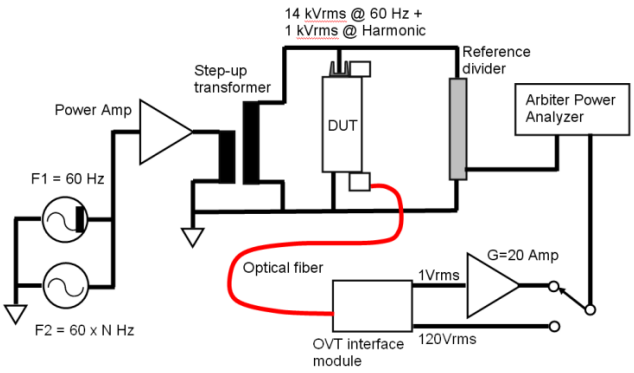

Figure 5. Schematic diagram of test setup used for harmonic response of the MetPod Voltage sensor and the OVT

The outputs of the interface module and the reference divider were fed into a power quality analyzer (Arbiter Systems 931A) with a maximum frequency of 3 kHz, or the 50th harmonic. The reported amplitude and phase are relative to the fundamental component present. Data were recorded by adjusting the harmonic amplitude to be 2% - 10% of the fundamental amplitude. The 60 Hz fundamental was kept constant at 14 kV. The amplitude error was typically +/- 0.05%, while the phase error was typically +/- 0.2 degrees.

B. Current Measurement Setup

The current response of the MetPod was measured by providing external 8VDC power to the MetPod through an auxiliary power input port that was installed for these tests. This allows the current sensor to be functional without having to apply high voltage to activate the power supply. A sine wave from an arbitrary waveform generator was amplified by a 2400W power amplifier, which then drove the primary winding of a 122:1 turns ratio, 22 kVA transformer. The transformer secondary was connected to a short length of stranded copper cable that formed 5 turns through the MetPod current sensor slot. An open-loop split-core sensor (LEM series HBT-200, 50 A/V, 50 kHz bandwidth) was used as the reference. The optical fiber output of the MetPod was coupled to the interface module to provide a low voltage reconstruction of 5 times the current in the conductor. The multiple turns were used to maintain adequate signal to noise ratio while operating the test setup at relatively low conductor currents (at high frequencies, the conductor current was <10 A).

The MetPod and reference signals were monitored with an HP 3478A true RMS multimeter, and phase angle was measured with a Krohn-Hite 6500 phase meter. The magnitude error with this test setup was typically +/- 0.5%, while the phase angle error was typically +/- 0.2 degrees. The phase error was extracted from the raw phase measurement by subtracting a baseline phase delay caused by the group delay of the optical fiber link. The delay resulted in a phase angle offset in degrees that is given by -0.23f, where f is the harmonic frequency in Hz. For example, the phase offset is -13.8 degrees at 60 Hz.

VII. TEST RESULTS

Results from the tests performed on above sensors are presented below. In all cases, the reported magnitude error or ratio is a relative to the magnitude of the measured harmonic. Since the harmonic signal amplitude in many cases is only a few percent of the fundamental signal, the reported errors are <0.1% of the total applied signal (fundamental + harmonic).

A. Voltage Measurement of OVT

The results for the OVT are shown in Figure 6 (amplitude) and Figure 7 (phase angle).

 ISBN: 978-1-61208-259-2

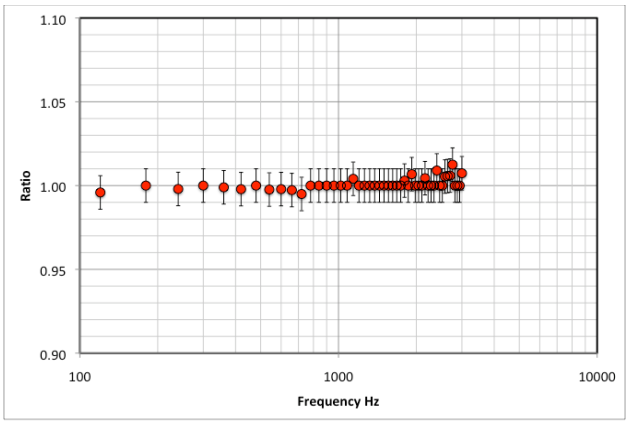

Figure 6. Amplitude response of OVT voltage sensor versus frequency

The OVT voltage sensor maintains 1% or better accuracy over the entire range of frequencies tested, up to 3 kHz or the 50th harmonic. The phase angle does not exceed 10 degrees lag at the 50th harmonic. The phase response can be modeled as a second-order low-pass system response with a bandwidth of 18 kHz.

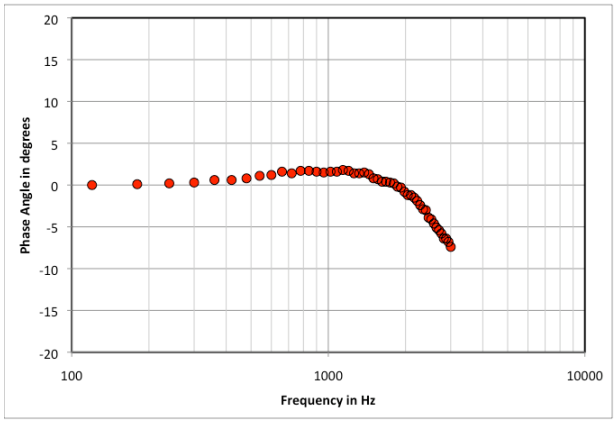

Figure 7. Phase response of OVT voltage sensor versus frequency

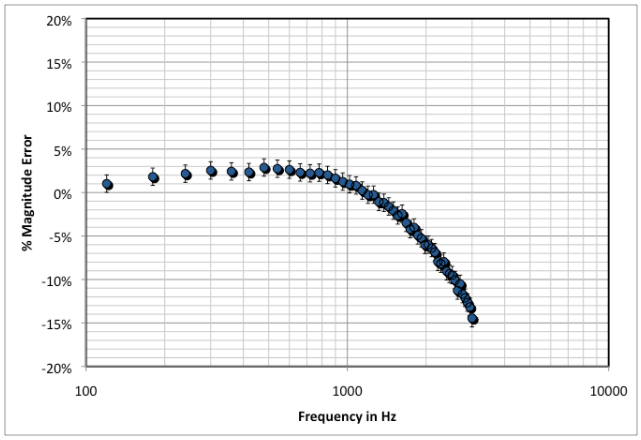

Figure 8. Amplitude response of MetPod voltage sensor versus frequency

B. *Voltage Measurement of MetPod*

The magnitude response versus frequency of the MetPod's voltage sensor using the 120 Vrms output from the interface module is shown in Figure 8, and the phase angle response is shown in Figure 9. The MetPod voltage sensor maintains better than 5% accuracy up to 1.8 kHz or the 30th harmonic of 60 Hz. The phase error remains less than 30 degrees at the 30th harmonic. The response indicates an overall 3 dB voltage sensor bandwidth of approximately 3.2 kHz. The bandwidth is currently limited by the interface module, and could be increased to the bandwidth of the digital optical link, or 20 kHz, if desired.

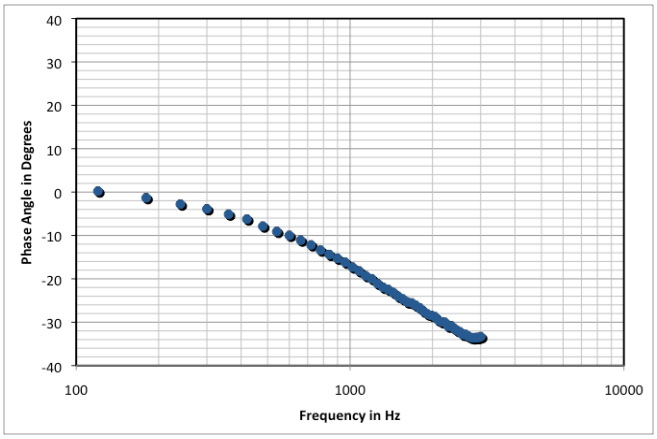

Figure 9. Phase response of MetPod voltage sensor versus frequency

C. *Current Measurement of MetPod*

The magnitude response versus frequency of the MetPod's current sensor is shown in Figure 10, and the phase angle in Figure 11.

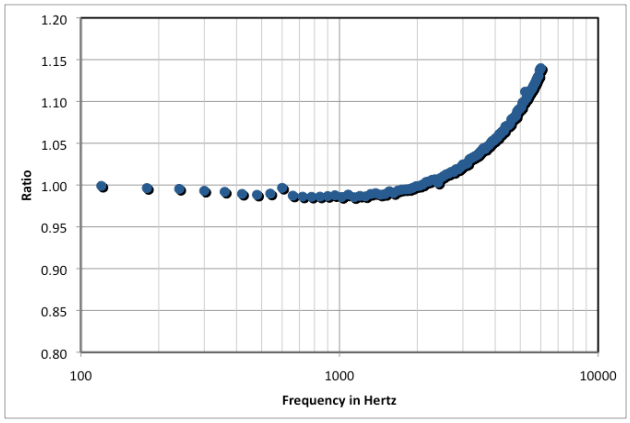

Figure 10. Amplitude response of MetPod current sensor versus frequency.

The magnitude accuracy of the current sensor remains within 5% at 4 kHz, which is the 66th harmonic of 60 Hz. The phase error remains within +/- 5 degrees up to 6 kHz, or the 100th harmonic.

 ISBN: 978-1-61208-259-2

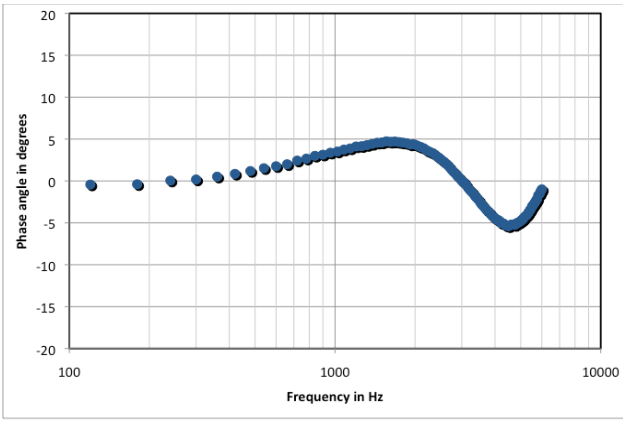

Figure 11. Phase angle versus frequency for MetPod current sensor

The MetPod current sensor frequency response was also evaluated by comparing the response with a reference CT (Ritz extended range, 0.15% from 1% - 150% I_{nom}, 1000:5) using the Arbiter 931A power quality analyzer. In this case, the applied voltage was purely fundamental 60 Hz at 14 kV, whereas the current was 100% at the harmonic frequency being tested. The response is shown in Figure 12.

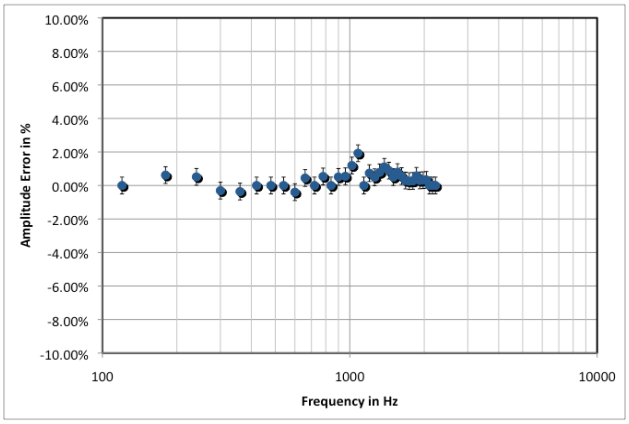

Figure 12. MetPod current sensor amplitude response versus harmonic frequency

The frequency response remains within 2% out to 2100 Hz, the highest frequency tested in this configuration.

VIII. CONCLUSIONS

Optical sensors are proving their value, especially in applications where accurate measurement over wider dynamic range is required, or where ability to retrofit, and improved safety are of main concern. They are suited for the advanced functionality of leading-edge protective relays and meters and for compatibility with digital communications in modern substations. Signal processing inside the current and voltage electronics of the sensor is inherently digital in nature and is accessible in a format consistent with IEC standards such as IEC 61850-9-1.

The intrinsic insulating properties of the non-conductive optical fiber allow the optical transducer to be used on 15 kV systems as well as 460 V systems. Because the optical sensors monitor the external electric or magnetic fields, they do not burden the generating system, resulting in savings by eliminating the electrical losses and production of heat within the monitoring system. The use of optical sensors brings several significant advantages such as:

- Reduced substation costs (combined VTs and CTs are suitable for both metering and protection).
- Reduced installation and commissioning costs (the sensor's lighter weight has a direct impact on foundation size, ease of equipment installation, and transportation and handling).
- Improved operating performance:
- Accuracy over a wide dynamic range,
- Intrinsically safe, no ferroresonance or open-circuit secondary concerns.
- Reduced maintenance and overhaul costs including reduced end of life disposal costs (no oil or SF6).

ACKNOWLEDGMENT

This work was partially supported by the Dept. of Energy SBIR Phase III Xlerator Program under contract DE-OE0000529.

REFERENCES

[1] F. Zavoda, "Advanced Distribution Automation (ADA) Applications and Power Quality in Smart Grids," CICED 2010, Nanjing, China, September 2010, pp. 1-7.

[2] B. K. Duncan and B. G. Bailey, "Protection, Metering, Monitoring and Control of Medium Voltage Power Systems," IEEE Transactions on Power Delivery, Vol. 40, No. 1, January/February, 2004, pp. 33-40.

[3] Handbook for Electricity Metering, 10th Edition, 2002 (Edison Electric Institute), pp. 381 – 391.

[4] T. W. Cease and P. Johnston , "A Magneto-Optic Current Transducer," IEEE Transactions on Power Delivery, Vol. 5, April 1990, pp. 548 – 555.

[5] J. Blake, P. Tantaswadi, and R. T. de Carvalho, "In-line Sagnac Interferometric Current Sensor," IEEE Transactions on Power Delivery, Vol. 11, January 1996, pp. 116 – 121.

[6] C. P. Yakymyshyn, S. Weikel, P. Johnston, and M. Brubaker, "362 kV Optical Voltage Transducer- Final Report," ESEERCO Research Report EP91-04, December, 1998.

[7] M. A. Brubaker, P. J. Hamilton, and C. P. Yakymyshyn, , "Clamp-On Untethered Power Interface Pod", U. S. Department of Energy, SBIR Grant Number DE-FG03-01ER832228/A002, Phase II Final Report, August, 2004.

[8] IEEE Standard Requirements for Instrument Transformers, IEEE Std. C57.13-1993.

[9] IEC 60044-7, Instrument Transformers, Part 7: Electronic Voltage Transformers, 1992-12.

 ISBN: 978-1-61208-259-2